Thirteenth International Symposium on Space Terahertz Technology, Harvard University, March 2002.

Generation of Millimetre and Sub-Millimetre Waves by Photomixing in a 1.55 μm wavelength Photodiode.

P. G. Huggard* & B. N. Ellison,
Rutherford Appleton Laboratory, Chilton,
Didcot, OX11 0QX, UK

P. Shen, N. J. Gomes & P. A. Davies,
Department of Electronics, University of Kent,
Canterbury, CT2 7NT, UK

W. P. Shillue, A.Vaccari & J. M Payne,
NRAO, Tucson, AZ 85721-0655, USA

Abstract: We report on the generation of radiation at frequencies from 70 GHz to above 600 GHz by photomixing in commercially available 70 GHz bandwidth photodiodes. The mm-wave and sub-mm-wave power was generated in W-band waveguide mounts by the beating of two 1.55 μm laser beams. Maximum optical to mm-wave power conversion efficiencies above 1 % were measured at frequencies between 75 GHz and 110 GHz, where an input power of +10 dBm yielded a non-saturated output power above -10 dBm. Measured output powers fell approximately as $(\text{frequency})^{-4}$ above 140 GHz, so that a power of approximately -40 dBm was detected at 625 GHz. We remark that the waveguide mount is non-optimised for frequencies above 110 GHz, and so these measurements represent a lower limit on the generated power.

Introduction: Photomixer, also known as photonic, sources generate power at the difference frequency of two visible or near infrared laser beams by using ultrafast photoconductors or photodiodes. We have constructed photomixers based upon commercially available 1.55 μm photodiodes [1] which have a 70 GHz analogue bandwidth, our objective being the provision of photonic sources for use as phase references, phase calibrators, and local oscillators for heterodyne receivers in the ALMA telescope [2].

The work presented below has extended previous W-band measurements on the photodiodes [3] by incorporating modified devices into a waveguide mount. Advantages of this approach include the ability to provide optimised photodiode-embedding circuit impedance match conditions, e.g. by the use of stub tuners, and the ease of interface with standard waveguide components. The stub tuner approach is particularly useful in the case of photodiode mm-wave sources, as the effects of large and sometimes uncertain capacitance on the high frequency roll-off of the responsivity can be reduced. Our findings on the advantages of this waveguide mount approach have already been reported [4, 5].

---

* e-mail: p.g.huggard@rl.ac.uk

In what follows, we describe how the 1.55 μm wavelength photodiodes were adapted for use in the specially designed W-band waveguide mount. We further report how the cleaved single mode optical fibre was fixed in position with respect to the photodiode chip to form a compact and mechanically stable mm-wave source. Results are presented showing the dependence of mm-wave power on optical input power and on applied bias. Although the mount is optimised for W-band frequencies, i.e. from 75 GHz to 110 GHz, and the diode bandwidth is below 100 GHz, we have been able to measure powers at frequencies from 70 GHz up to the optical source imposed limit of 625 GHz. Finally, we demonstrate the reproducibility of the design by comparing the W-band characteristics of two photomixers for fixed backshort tuning.

The photomixing source and apparatus: The p-i-n photodiodes utilised are epitaxially grown on InP and are supplied as chips 2 mm in length and 500 μm in width. Incident 1.55 μm radiation is injected through an antireflection-coated facet and passes via a rib waveguide to the 5 μm x 20 μm photodiode [6]. The photodiode output contact is connected to the centre conductor of a short length of 50 Ω coplanar waveguide. Manufacturer's data indicates an external DC responsivity about 0.4 A/W at a reverse bias of 1V with a bandwidth of 70 GHz in a 50 Ω environment [6].

Our waveguide photomixer approach requires that the photodiode chip is enclosed in a metal channel. The cross-sectional dimensions of the supplied photodiode substrate are relatively large compared to the operational wavelength and longitudinal propagation of radiation in a waveguide mode may occur for frequencies above 94 GHz. Propagation of such a mode in the channel would represent a loss of power from the desired TE_{10} mode in the WR-10 output waveguide. To address this problem the chips were mechanically thinned to 200 μm and reduced in width to 380 μm: this modification increases the cut-off frequency of the undesired mode to 145 GHz.

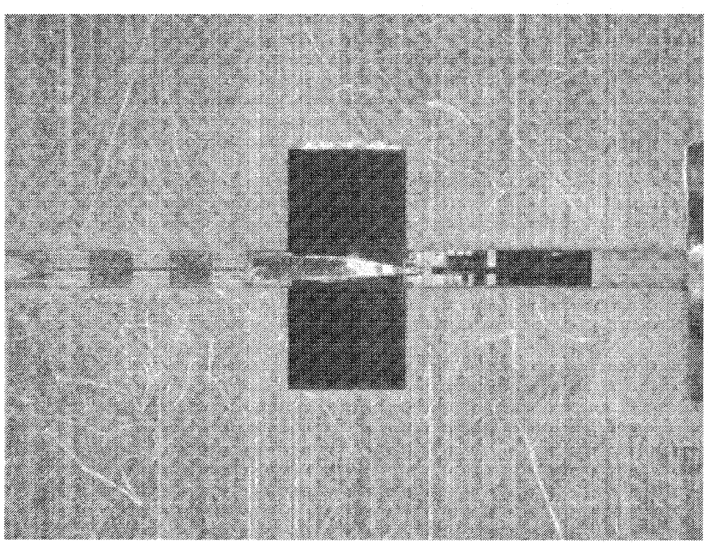

Figure 1: Photograph of u^{2}t photodiode chip (right centre) incorporated in a photonic mixer block.

A modified chip, appearing as the predominantly black area on the centre right of Figure 1, was fixed in the channel of a photomixer block. The dark rectangular area in the middle of the photograph is the end of the WR-10 waveguide. Constant voltage bias is applied to the photodiode by means of a radio frequency choke structure defined on a 200 μm thick quartz substrate. This is visible on the left hand side of Figure 1. A wedge shaped gold foil extends across the WR-10 waveguide to make contact with the output conductor on the photodiode chip. The electrical connection between the photodiode contacts and the foil probe is made by means of low melting point InSn solder.

A single mode optical fibre transports the 1.55 μm radiation to the photomixer. The stripped fibre enters the photodiode channel from the right-hand side as viewed in Figure 1 and its cleaved end is positioned about 40 μm from the chip facet. The fibre is glued into a stainless steel ferrule, which passes through a hole in the block and is then clamped to an x-y-z positioner. When alignment between fibre and chip has been optimised, the ferrule is fastened to the photomixer block by epoxy resin. After this has cured, the rigidity of the bond is such that light finger pressure on the exposed ferrule does not disturb the fibre to chip alignment.

In use, the photomixer block is capped with a metal lid through which the rectangular waveguide continues. A sliding backshort in this waveguide may be adjusted by means of a micrometer screw: Figure 2. To give an idea of scale, the rectangular block dimensions are 20 mm x 22 mm x 7 mm. The micrometer adjustment mechanism for the backshort could be eliminated in a future fixed backshort production device, considerable reducing the source height. This figure also shows the SMA bias connector and the epoxied stainless steel ferrule that supports the soft buffer coated fibre.

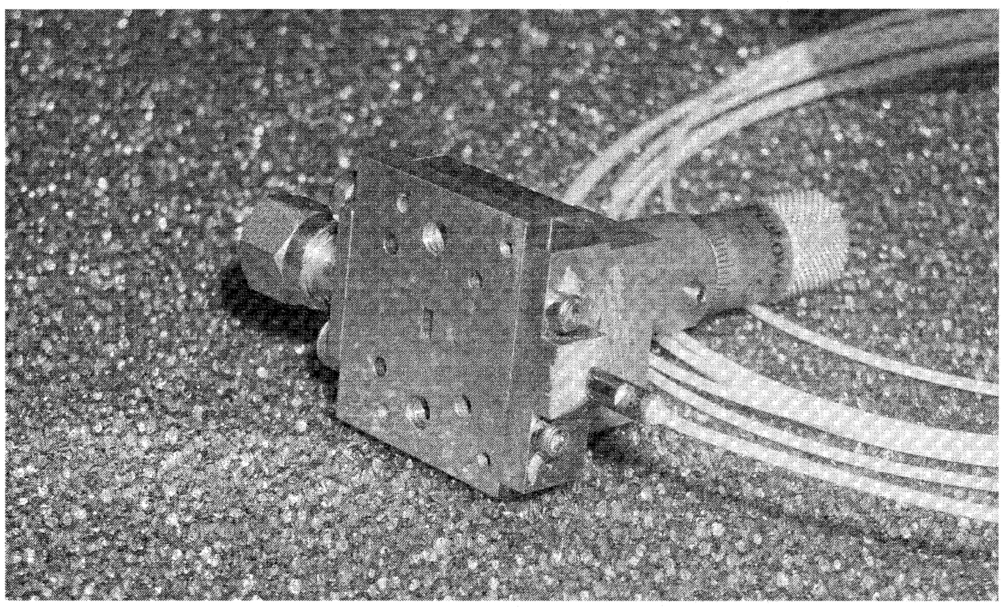

Figure 2: Photograph of completed photonic sources showing theWR-10 output waveguide and the stainless steel fibre ferrule cemented to the block. The block base dimensions are 20 mm x 25 mm.

Optical power is provided by two 1.55 μm diode lasers whose outputs are combined into a single mode fibre. The lasers and associated microprocessor driven control electronics have been packaged into a single microprocessor controlled 19" rack unit by NRAO. Frequency offsets from 1 GHz to 625 GHz and a combined output power above +10 dBm are available.

Methods used to characterise the generated mm-wave power depended on the frequency. An external W-band mixer connected to a spectrum analyser was used for frequencies from 75 GHz to 200 GHz. Measured in-band powers were verified to within 1 dB by means of a thermocouple power meter. At higher frequencies the radiation was coupled into free space by a rectangular feedhorn antenna. For power measurement the radiation was focussed into a calibrated Golay cell by a HDPE lens. Alternatively, for frequency verification outside the range of the spectrum analyser, the mm-wave signal was coupled into a Fourier transform spectrometer: this confirmed that the radiation was emitted at the difference frequency of the laser beams, and any higher harmonic components could not be discerned from the measurement noise floor.

Experimental results and discussion: The DC external responsivity of the photodiode was measured as 0.4 A/W for a reverse bias of 1.2 V, in good agreement with the manufacturer's specification. Figure 3 presents the dependence of the mm-wave power on optical power at frequencies of 75 GHz and 100 GHz for a reverse bias of –1.2 V. In both cases the expected square law response is observed, as indicated by the lines which have a slope of two. Respective maximum mm-wave powers of –7.7 dBm (170 μW) and –10 dBm (100 μW) are obtained for the maximum excitation power of +10 dBm (10 mW). These values correspond to a power conversion efficiency of at least 1%. The data shows no evidence of saturation and so mm-wave powers of at least 0 dBm would be expected if this behaviour continues to the optical power limit of +16 dBm (40 mW). For comparison purposes, powers of +10 dBm have recently been generated by strongly saturated uni-travelling-carrier photodiodes [7] driven by mode locked laser pulses. The pulse repetition frequency was 100 GHz and the average photocurrent was about 30 mA. Photomixing experiments in waveguide mounts with these photodiodes at the same frequency yields +3 dBm (2 mW) for an input of +23 dBm (200 mW) [8].

The bias dependence of the power at 100 GHz is shown in the Figure 3 inset for an optical power of +8 dBm. The signal initially increases strongly as the bias is changed from forward to reverse, and the power then saturates for reverse biases above 0.5 V. The total contrast available by varying the bias by 1.4 V is about 10 dB. Decreasing reverse bias increases the junction capacitance and possibly also increases the carrier transit time. Both these effects reduce the overall detector bandwidth – see below - and hence the mm-wave power at a given frequency decreases. This bias sensitivity offers the facility to remotely control photomixer output powers, a useful feature if the photomixer is to be used as a local oscillator for SIS mixers.

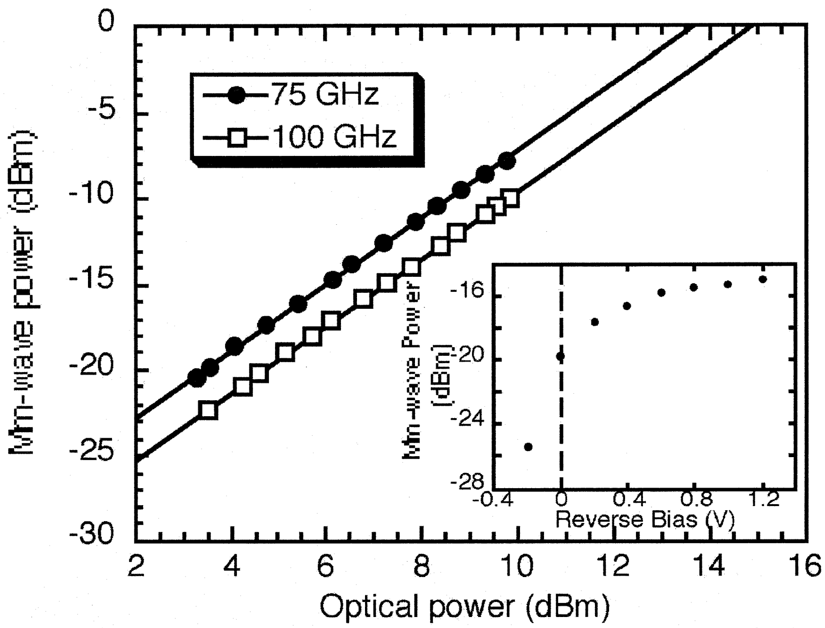

Figure 3: Dependence of mm-wave power on optical power at frequencies of 75 GHz (solid circles) and 100 GHz (open squares) for a reverse bias of –1.2 V. The lines indicate a slope of two. The inset shows the dependence of the mm-wave power on bias at a frequency of 100 GHz and an optical power of +7.8 dBm (6 mW).

While measuring the above power dependences, the position of the backshort was optimised at each frequency. Figure 4 displays the dependence of this maximised power as a function of frequency between 75 GHz and 625 GHz. The measurements were made at a reverse bias of 1 V and for a constant +10 dBm optical input power. The mm-wave power is found to peak at around –10 dBm for frequencies close to 100 GHz. A sharp dip is observed in the region of 120 GHz, above which the power recovers and then decreases approximately proportional to $(\text{frequency})^{-4}$ so that the detected power above 600 GHz is about –40 dBm (100 nW).

The frequency response of the photomixer is determined by both photodiode properties and by the characteristics of the photomixer block and coupling structure. The photodiode bandwidth is a combination of the RC bandwidth (100 GHz) and the carrier transit time, τ_d, limited bandwidth (110 GHz) [6]. The expected dependence of microwave power on frequency, P(f), is thus a product of two terms, both varying as f^{-2} at high frequencies [9]:

$$P(f) \propto \frac{1}{[1+(2\pi f\tau_d)^2][1+(2\pi fRC)^2]} \qquad (1)$$

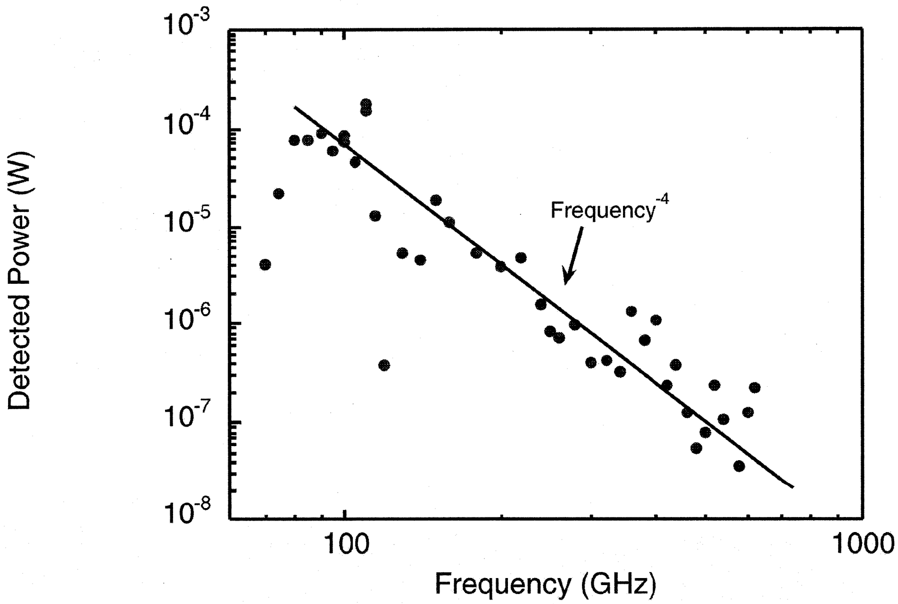

Figure 4: Dependence of mm-wave power on frequency for a constant excitation power of +10 dBm (10 mW). The line is a guide to the eye and indicates a $(\text{frequency})^{-4}$ dependence.

Within the band of the photomixer block, 75 GHz to 110 GHz, the effects of capacitance on the roll-off with frequency can be reduced by tuning the backshort appropriately. This tuning become less effective as the frequency rises and the waveguide becomes overmoded. HFSS calculations show that radiation can propagate in the photodiode and choke channels for frequencies above 150 GHz: this is a potential further loss mechanism. In addition the feedhorn beam pattern is unknown at high frequencies and the efficiency of coupling generated power to the Golay cell detector may therefore be lower. All these factors are tend to reduce the detected power and thus the data displayed in Figure 4 actually represents a lower limit on the available mm-wave power. We note that a power above –30 dBm is available at frequencies up to 300 GHz. This power level demonstrates the suitability of this non-optimised photomixer, when driven by an appropriately phase locked laser system, as a local oscillator source for an SIS mixer up to 300 GHz.

We mention that the sharp dip in the spectrum at about 120 GHz is probably a consequence of placing the photodiode close to the waveguide wall and contacting to it by means of a probe extending across the guide. The equivalent circuit of this geometrical arrangement is a series LC combination in parallel with the photodiode [10]. This LC circuit has a short circuit resonance in full height waveguide at approximately twice the cut-off frequency of the TE_{10} mode. For our WR-10 waveguide the cut-off frequency is about 59 GHz, and thus the dip position is consistent with this explanation. This undesirable drop in output power can be eliminated by reducing the height of the waveguide or by positioning the source centrally in the waveguide [11].

Finally, to demonstrate the reproducibility of our design, we compare the performance of two photomixers: Figure 5. This graph shows the performance of the two sources for a fixed backshort tuning which maximised the 90 GHz power. One photomixer (red squares) was driven by the University of Kent laser system [4] and the second (blue circles) was used in the study with the NRAO source described above. The output spectra are similar in shape over most of the waveguide band, although some difference can be seen above 100 GHz. Output powers from the first mixer have been scaled by a few dB to achieve a better overlap of the curves. The discrepancy between curves is not surprising given differences between the laser systems, the responsivities of photodiodes and the manual assembly methods used to shape the probe, assemble the devices and position the fibre. We envisage that a production photomixer should incorporate a photolithographically defined probe on a quartz substrate which would present an impedance matched load to the photodiode. This should assist the production of photomixers with similar performances and with a lower W-band frequency dependence.

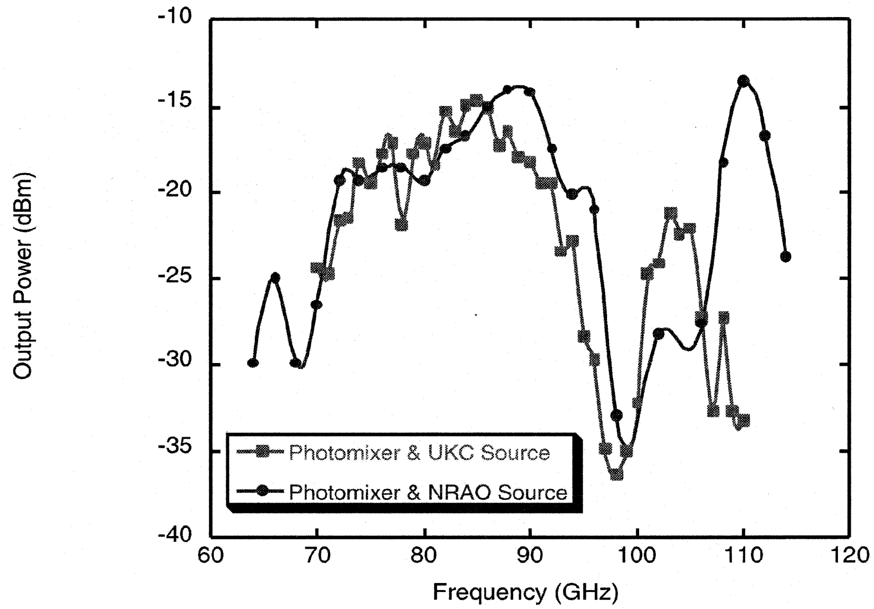

Figure 5: Comparison of the W-band tuning of two photomixers, both of which were fixed tuned for optimum power at 90 GHz. For comparison purposes the red data points have been scaled by a few dB to better overlap the blue points. The curves are a guide to the eye.

Conclusion: Ultrafast photodiodes have been coupled to rectangular W-band waveguide in a specialised mounting incorporating a tuneable backshort. Non-saturated peak powers above –8 dBm (-10 dBm) were generated at frequencies of 75 GHz (100 GHz) with power conversion efficiencies above 1%. The reproducibility of our design has been confirmed by comparing the performance of two fixed tuned devices. Output powers resulting from optimised tuning were found to decrease strongly with increasing frequency, dropping from about –10 dBm at 100 GHz to a level of –40 dBm at 625 GHz. The trend of the data indicates that the power depends approximately on $(\text{frequency})^{-4}$. Although the mount is not optimised for frequencies in the 200 GHz to 300 GHz range, we believe that the –30 dBm of power detected is already sufficient for the device to be used as a LO source for an SIS mixer.

References:

1: u^{2}t Innovative Optoelectronic Components GmbH, Tangermünder Weg 18, D13583 Berlin, Germany

2: J. M. Payne, W. P. Shillue and A. Vaccari, "Photonic Techniques for Use on the Atacama Large Millimeter Array", *Proc. Int. Topical Meeting Microwave Photonics*, Melbourne, pp. 105 - 108, IEEE (1999).

3: Bill Shillue, "Millimeter-wave RF Power measurements of a Commercial Photomixer", *ALMA Memo Series* #313: http://www.alma.nrao.edu/memos/index.html.

4: P. G. Huggard, B. N. Ellison, P. Shen, N. J. Gomes, P. A. Davies, W. P. Shillue, A.Vaccari and J. M Payne, "Efficient generation of guided millimetre-wave power by photomixing", *IEEE Photonics Tech. Lett.* **14**, pp. 197-199 (2002).

5: P. G. Huggard, B. N. Ellison, P. Shen, N. J. Gomes, P. A. Davies, W. P. Shillue, A.Vaccari and J. M Payne, "Generation of millimetre and sub-millimetre waves by photomixing in a 1.55 μm wavelength photodiode", *Electronics Lett.* **38**, pp. 327-328 (2002).

6: D. Trommer, A. Umbach and G. Unterbörsch "InGaAs Photodetector with Integrated Biasing network for mm-Wave Applications", *Proc. 10th Int. Conf. Indium Phosphide and Related Materials (IPRM'98),* Tsukuba, pp. 276 – 279, IEEE (1998).

7: T. Nagatsuma, T. Ishibashi, A. Hirata, Y. Hirota, T. Minotani, A. Sasaki and H. Ito: "Characterisation of a uni-travelling-carrier photodiode monolithically integrated with a matching circuit", *Electronics Lett.* **37**, pp. 1246 – 1247 (2001); H. Ito, Y. Hirota, A. Hirata, T. Nagatsuma and T. Ishibashi: "11dBm photonic millimetre-wave generation at 100 GHz using uni-travelling-carrier photodiodes", *Electronics Lett.* **37**, pp. 1225 – 1226 (2001)

8: T. Noguchi, A. Ueda, H. Iwashita, Y. Sekimoto, M. Ishiguro, T. Ishibashi, H. Ito and T. Nagatasmua, "A photonic local oscillator for an SIS mixer in the 100 GHz band", these proceedings.

9: E. R. Brown, F. W. Smith and K. A. McIntosh, "Coherent millimeter-wave generation by heterodyne conversion in low-temperature-grown GaAs", *J. Appl. Phys.* **73**, pp. 1480 - 1484 (1993).

10: A. R. Kerr, "Low noise room-temperature and cryogenic mixers for 80-120 GHz", *IEEE Trans. Microwave Theory Tech.* **43**, pp. 781 - 787 (1975).

11: T.H. Büttgenbach, T.D. Groesbeck, and B.N. Ellison, "A Scale Mixer Model for SIS Waveguide Receivers", Int J. Infrared Millimeter Waves **11**, pp. 1 -20 (1990).